bioRxiv preprint doi: https://doi.org/10.1101/2021.05.17.444590; this version posted May 18, 2021. The copyright holder for this preprint (which was not certified by peer review) is the author/funder. All rights reserved. No reuse allowed without permission.

1 The association of human astrovirus with extracellular vesicles facilitates cell
2 infection and protects the virus from neutralizing antibodies
3
4 Baez-N, Carlos[a], Iván R. Quevedo[b], Susana López[a], Carlos F. Arias[a], Pavel Iša[a]#
5
6 [a] Departamento de Genética del Desarrollo y Fisiología Molecular, Instituto de
7 Biotecnología, Universidad Nacional Autónoma de México, Cuernavaca, Morelos,
8 Mexico
9 [b] Departamento de Ingeniería Química, Industrial y de Alimentos, Universidad
10 Iberoamericana, Ciudad de México, México
11
12 Running title: Human astrovirus associates with extracellular vesicles.
13
14
15 #Address correspondence to: Pavel Iša, pavel.isa@ibt.unam.mx
16
17
18 Keywords.
19 Astrovirus, extracellular vesicles, vesicle mediated infection,
20

bioRxiv preprint doi: https://doi.org/10.1101/2021.05.17.444590; this version posted May 18, 2021. The copyright holder for this preprint (which was not certified by peer review) is the author/funder. All rights reserved. No reuse allowed without permission.

Abstract

Viral gastroenteritis has a global distribution and represents a high risk for vulnerable population and children under 5 years because of acute diarrhea, fever and dehydration. Human astroviruses (HAstV) have been identified as the third most important cause of viral gastroenteritis in pediatric and immunocompromised patients. Furthermore, HAstV has been reported in biopsies taken from patients with encephalitis, meningitis and acute respiratory infection, yet it is not clear how the virus reaches these organs. In this work we tested the possibility that the released astrovirus particles could be associated with extracellular vesicles. Comparison between vesicles purified from astrovirus- and mock-infected cells showed that infection with HAstV Yuc8 enhances production of vesicles larger than 150 nm. These vesicles contain CD63 and Alix, two markers of vesicular structures. Some of the extracellular virus was found associated with vesicular membranes, and this association facilitates cell infection in the absence of trypsin activation and protects virions from neutralizing antibodies. Our findings suggest a new pathway for HAstV spread and might represent an explanation for the extraintestinal presence of some astrovirus strains.

Importance.

Astroviruses are an important cause of diarrhea in children; recently some reports have found these viruses in extra-intestinal organs, including the central nervous system, causing unexpected clinical disease. In this work we found that human astrovirus strain Yuc8 associates with extracellular vesicles, possibly during or after their cell egress. The association with vesicles seems to increase astrovirus infectivity in less susceptible cells, and renders virus particles insensitive to neutralization by antibodies. These data suggest that extracellular vesicles could represent a novel pathway for astrovirus to disseminate outside the gastrointestinal tract.

bioRxiv preprint doi: https://doi.org/10.1101/2021.05.17.444590; this version posted May 18, 2021. The copyright holder for this preprint (which was not certified by peer review) is the author/funder. All rights reserved. No reuse allowed without permission.

52 **Introduction**

53 Astroviruses are considered the third most important cause of viral
54 gastroenteritis in children, as well as in the young of many animal species (1, 2).
55 Moreover, in some mammalian species astroviruses have been associated with
56 different neurological disorders and have been found in biopsies of patients with
57 encephalitis, meningitis or acute respiratory infections (1, 2). Given that mammalian
58 astroviruses are considered intestinal viruses, the central question is: "How could
59 astroviruses get into the central nervous system and respiratory tract?" (3).

60 From the structural point of view, astroviruses are small non-enveloped
61 viruses, forming the family *Astroviridae*. They contain a single-stranded, positive
62 sense RNA (ssRNA+) genome whose length ranges, in the case of mammalian
63 astroviruses, from 6.1 to 6.8 kb. The astrovirus genome is organized into three open
64 reading frames, named ORF1a, ORF1b and ORF2, which encode non-structural
65 (ORF1a and ORF1b) and structural (ORF2) viral proteins (4, 5). Astrovirus cell entry
66 is not completely understood, and the virus cell surface receptor is unknown,
67 although the fact that the susceptibility of different cell lines to infection with
68 astrovirus depends on the viral serotype (6-8), suggests that there could be more
69 than one receptor. Astrovirus enters into cells by clathrin-mediated endocytosis and
70 it seems that entry process follows a classical route into late endosomes (4, 9).
71 During maturation, the astrovirus particles are subjected to distinct proteolytic
72 processes. First, the capsid protein VP90 of the newly assembled astrovirus particles
73 is cleaved intracellularly by caspases to give immature virions composed by the viral
74 protein VP70. This cleavage is associated with the release of the viral particles from
75 the infected cell (10, 11). Then, once in the extracellular medium, the virion is
76 processed by trypsin-like extracellular proteases to render infectious, mature virions,
77 composed by the final protein products VP27 and VP34 (12, 13).

78 One of the less characterized phases of the astrovirus replication cycle, is cell
79 egress. It has been proposed that astrovirus release is a non-lytic process, during
80 which the extracellular virions appear to be associated with membranous structures
81 (11, 14). In this regard, it is of interest that the cell exit of different viruses has been
82 associated with extracellular vesicles (EV) (15-17). EV are a heterogeneous group

bioRxiv preprint doi: https://doi.org/10.1101/2021.05.17.444590; this version posted May 18, 2021. The copyright holder for this preprint (which was not certified by peer review) is the author/funder. All rights reserved. No reuse allowed without permission.

83 of small vesicles with a lipidic bilayer, ranging from 50 nm to 1,000 nm of diameter
84 (18). These vesicles are secreted by different types of cells and can be isolated from
85 conditioned media of cultured cells, as well as from virtually any type of body fluid,
86 including blood, urine, ascites, bronchoalveolar lavage, saliva and cerebrospinal
87 fluid (19, 20). There are different types of EV, with exosomes being the better
88 characterized, having a diameter of around 50 to 150 nm, and also well studied
89 microvesicles with diameter around 50 to 1,000 nm. Exosomes originate from the
90 endosomal compartment by fusion of multivesicular bodies with the plasma
91 membrane, while microvesicles originate from the plasma membrane by outward
92 budding (21).

93 Viral infections affect cell physiology, as well as many cellular processes,
94 including protein synthesis and degradation (22, 23), intracellular trafficking and
95 vesicle secretion (16, 24, 25). In the last few years the evidence regarding the
96 interaction between EV and different types of viruses (26-28) has accumulated.
97 Particularly, several positive-sense ssRNA viruses, like hepatitis C virus (HCV) and
98 hepatitis E virus (HEV), have been found to associate with EV or to use the
99 mechanism of EV biogenesis as an egress pathway (29-32). In addition, DNA
100 viruses like HSV-1 (33) and JC polyomavirus (34) also have been observed
101 interacting or being released with EV.

102 Given the possibility that EV could be involved in the human astrovirus
103 (HAstV) cell egress, we tested the possibility that astrovirus particles could be
104 released in association with this type of vesicles. To characterize the possible
105 interaction between EV and the virus, Caco-2 cells were infected with the Yuc8 strain
106 of HAstV and EV were purified from the cell culture media by differential
107 centrifugation coupled to polyethylene glycol 6000 (PEG) precipitation and affinity
108 magnetic sorting. Our results suggest that astrovirus infection stimulates the
109 secretion of EV and astrovirus particles seem to associate with EV. These vesicle-
110 associated viruses acquire the ability to infect cells in the absence of trypsin
111 activation. Also, viral particles associated with EV were refractory to the effect of
112 neutralizing antibodies, suggesting that EV are able to protect the virions from this
113 interaction.

bioRxiv preprint doi: https://doi.org/10.1101/2021.05.17.444590; this version posted May 18, 2021. The copyright holder for this preprint (which was not certified by peer review) is the author/funder. All rights reserved. No reuse allowed without permission.

114

115 ## Materials and methods

116

117 ### Cell lines, virus, reagents and antibodies

118 Human colon adenocarcinoma cells (Caco-2), and rhesus monkey epithelial
119 cells (MA104), were obtained from American type culture collection (ATCC,
120 Manassas, VA, USA). Dulbecco modified Eagle medium - high glucose (DMEM) was
121 purchased from Sigma Aldrich (San Luis, MI, USA), while Advanced-DMEM (A-
122 DMEM), fetal bovine serum (FBS) and trypsin were from Gibco (Thermo Fisher
123 Scientific, USA). Triton X-100 was acquired from Boehringer Mannheim, (Germany),
124 whereas Polyethylene glycol 6000, soybean trypsin inhibitor and Minimum Essential
125 Medium (MEM) were acquired from, Sigma-Aldrich (San Luis, MI, USA).
126 Formaldehyde was obtained from J.T. Baker, (USA), and MagCapture™ exosome
127 isolation kit PS was from FUJIFILM Wako Pure Chemical Corporation (Osaka,
128 Japan). Human astrovirus serotype 8, strain Yuc8 was originally isolated in our
129 laboratory (35). Polyclonal rabbit antibody specific for Yuc8 virus (anti-Yuc8) was
130 prepared in our laboratory (11). Rabbit polyclonal antibodies specific for anti-CD63
131 and anti-Alix were acquired from Santa Cruz (Santa Cruz Biotechnology, CA, USA),
132 and Aviva Systems Biology (Aviva Systems Biology, CA, USA) respectively, while
133 monoclonal antibody specific to anti- protein disulfide isomerase (PDI, clone 1D3)
134 was obtained from Enzo Life Sciences, Inc (C. Mexico, Mexico). Anti-rabbit
135 peroxidase conjugated antibody was from KPL (MD USA), and protein A, peroxidase
136 conjugate was from Sigma Aldrich (Sigma Aldrich).

137

138 ### Cell culture and viral propagation

139 Caco-2 cells were cultured in DMEM supplemented with non-essential amino
140 acids and 15% heat-inactivated FBS, in a 10% CO_2 atmosphere at 37°C (14). MA104
141 cells were grown in A-DMEM, supplemented with 5% FBS, at 37°C in a 5% CO_2
142 atmosphere (36).

143 A working stock of human astrovirus serotype 8, strain Yuc8 (35), was
144 prepared as previously described (37). The virus was activated just prior to infection

bioRxiv preprint doi: https://doi.org/10.1101/2021.05.17.444590; this version posted May 18, 2021. The copyright holder for this preprint (which was not certified by peer review) is the author/funder. All rights reserved. No reuse allowed without permission.

145 with 200 µg/mL of trypsin, for 1 hour at 37 °C, followed by inactivation with 200 µg/mL
146 of soybean trypsin inhibitor. Before infection, Caco-2 cell monolayers were washed
147 with MEM and incubated with activated virus for 1 hour at 37 °C. Then, cell
148 monolayers were washed twice with MEM, to remove non-adsorbed virus. Finally,
149 MEM was added to the cells, and infection was left to proceed for 48 hours at 37 °C.
150 Astrovirus particles were purified essentially as described previously (38).
151 Briefly, Caco-2 cells were infected with HAstV serotype 8 (Yuc8) at an MOI of 5 as
152 described above and the infection was left to proceed for 48 hours. After this time
153 cells were detached, and frozen and thawed three times. Then, cellular lysate was
154 clarified by centrifugation at 2,000 g for 10 minutes and then passed through a 0.45
155 µm filter (Milipore). Filtered supernatants were pelleted at 60,000 g for 16 hours at
156 4 °C in a SW28 Ti rotor (Beckman), and the resulting pellet was resuspended in TNE
157 buffer (50 mM Tris-HCl [pH 7.4], 0.1 M NaCl, 10 mM EDTA). This suspension was
158 adjusted to 0.5% v/v with octyl glucoside in TNE buffer and incubated for 30 minutes
159 on ice. Finally, virus was pelleted through a 30% w/v sucrose cushion in TNE buffer
160 for two hours at 200,000 g in a SW55 Ti Beckman rotor. The pelleted viral particles
161 were resuspended in TNE buffer.
162
163 **Viral infectivity assay**
164 Viral titers were determined by immuno-peroxidase staining to detect
165 infectious focus forming units (FFU) as described previously (11, 39). In brief, Caco-
166 2 cells were cultured to confluence in 96 wells plates and washed with serum-free
167 MEM before infection. Viral samples were activated with trypsin (200 µg/mL), for 1
168 hour at 37 °C, soybean trypsin inhibitor was added (200 µg/mL), and serial fold
169 dilutions of activated viral samples were performed. Diluted samples were added to
170 each well and let to adsorb for 1 hour at 37 °C. After adsorption period, the virus
171 inoculum in each well was removed, cells were washed twice with MEM and infection
172 was left to proceed in fresh MEM for 18 hours at 37°C. Cells were fixed for 20
173 minutes with 2% formaldehyde in phosphate-buffered saline (PBS), then they were
174 washed three times with PBS and permeabilized by a 15 minutes incubation with
175 0.2% Triton-X100 solution in PBS. Finally, cells were washed again three times with

bioRxiv preprint doi: https://doi.org/10.1101/2021.05.17.444590; this version posted May 18, 2021. The copyright holder for this preprint (which was not certified by peer review) is the author/funder. All rights reserved. No reuse allowed without permission.

176 PBS and incubated with a polyclonal rabbit anti-Yuc8 overnight at 4°C. Next day
177 cells were washed out three times with PBS and incubated with peroxidase
178 conjugated protein A for 2 hours at 37°C. After washing protein A, infected cells were
179 revealed by carbazole precipitation and FFU were counted.
180

181 **Kinetics of viral release**

182 Caco-2 cells were grown to confluence in 24 wells plates. Cell monolayers
183 were washed twice with MEM and infected with activated HAstV Yuc8 strain (at an
184 MOI of 5). Supernatants were harvested at three hours intervals starting at 12 hours
185 post infection (hpi) until 24 hpi, and centrifuged for 5 minutes at 500 g to separate
186 cellular debris. At the same time, MEM was added to cellular monolayers and cells
187 were lysed by two cycles of freeze-thaw. Infectious viral particles associated to cells
188 and present in supernatants were determined by an immune-peroxidase assay as
189 described above. Before trypsin activation, samples were incubated for 30 minutes
190 at 37°C with MEM or with 0.1% Triton X-100 diluted in MEM.
191

192 **Purification of extracellular vesicles**

193 Caco-2 cells, grown to confluence in 150 cm^2 flasks, were washed twice with
194 MEM and infected with trypsin activated HAstV Yuc8 at an MOI of 5. As a control,
195 cells were mock infected using an identical protocol without virus. Supernatants were
196 harvested at 18 hpi and processed by differential centrifugation essentially as
197 described before (40, 41). Briefly, supernatants were centrifuged at 500 g for five
198 minutes to obtain pellet 1 (P1), and the supernatant was again centrifuged at 2,000
199 g for 30 minutes, obtaining the pellet 2 (P2). The remaining supernatant was
200 centrifuged at 20,000 g for one hour, producing pellet 3. Finally, the last supernatant
201 was mixed with an equal volume of a solution of 16% polyethylene glycol 6000 (PEG),
202 1 M sodium chloride and left overnight at 4°C. The mixture was then centrifugated
203 at 10,000 g for one hour, yielding pellet 4. As proposed by a theoretical analysis of
204 sedimentation (42), the purified fraction in pellet 3 was considered to contain large
205 extracellular vesicles (LEV), while the fraction of pellet 4 contains small extracellular
206 vesicles (SEV). All centrifugations were performed at 4 °C and all pellets were

bioRxiv preprint doi: https://doi.org/10.1101/2021.05.17.444590; this version posted May 18, 2021. The copyright holder for this preprint (which was not certified by peer review) is the author/funder. All rights reserved. No reuse allowed without permission.

207 resuspended in sterile PBS. Virus titer in purified fractions was determined by
208 immune-peroxidase assay, with and without TX-100 treatment as described above
209 for supernatants in the assays of viral release kinetics.

210 For some experiments, in order to remove possible contaminants (i.e., free
211 contaminating virions or protein aggregates) from purified vesicles in LEV or SEV
212 fractions (pellets 3 and 4, respectively), the vesicle fractions were additionally
213 purified using the MagCapture^{TM} exosome isolation kit PS, according to the
214 manufacturer protocol.

215

216 **Immunodetection of cellular and viral proteins**

217 The fractions purified by differential centrifugation from supernatants of
218 infected and mock-infected Caco-2 cells were mixed with Laemmli sample buffer (50
219 mM Tris, pH 7.5, 2% SDS, 2% β-mercaptoethanol, 10 mM EDTA and 0.1%
220 bromophenol blue), boiled for 5 min and the proteins were separated by sodium
221 dodecyl sulfate-polyacrylamide gel electrophoresis (SDS-PAGE). Proteins were
222 transferred to a nitrocellulose membrane (Millipore, Bedford, MA, USA). Membranes
223 were blocked with 5% non-fat dried milk in PBS. The proteins of interest were
224 detected with specific primary antibodies followed by incubation with secondary
225 peroxidase-conjugated reagents. Primary antibodies were incubated with
226 membranes overnight at 4°C, washed three times with PBS 0.1% Tween (PBS-T)
227 and incubation continued with peroxidase conjugated secondary antibody or protein
228 A for 90 min, at room temperature. After these incubations the membranes were
229 washed again with PBS-T and proteins were visualized by Western Lightning
230 Chemiluminescence Reagent Plus (Perkin Elmer).

231

232 **Infectivity associated to the extracellular vesicles**

233 Fractions were purified from supernatant of astrovirus infected Caco-2 cells
234 by differential centrifugation coupled with isolation with magnetic beads
235 (MagCapture^{TM} exosome isolation kit PS), as described above. Vesicle containing
236 fractions were diluted in MEM and added to Caco-2 and MA104 cells, grown to
237 confluence in 96 wells plates, washed twice with MEM before addition. The fractions

bioRxiv preprint doi: https://doi.org/10.1101/2021.05.17.444590; this version posted May 18, 2021. The copyright holder for this preprint (which was not certified by peer review) is the author/funder. All rights reserved. No reuse allowed without permission.

238 were subjected to the following treatments before adsorption: with 0.1% Triton X-
239 100 for 30 minutes at 37°C; or were preincubated with an anti-Yuc8 neutralizing
240 antibody for 1 hour at 37°C; or by an incubation with 0.1% Triton X-100 for 30
241 minutes at 37°C, followed by neutralization with anti-Yuc8 antibody (1 hour at 37°C).
242 Control, non-treated samples were incubated in the same conditions but using an
243 equivalent volume of FBS-free MEM instead of Triton X-100 and/or anti-Yuc8
244 antibody. Vesicles were left to adsorb to cells during 2 hours at 37°C, then cells were
245 washed, fresh medium was added and the infection was left to proceed for 18 hours.
246 To test the capacity of purified EV to promote infection with externally bound
247 virus particles, LEV and SEV vesicles were purified from non-infected Caco-2 cells
248 as described above, including the isolation step with the MagCapture^{TM} exosome
249 isolation kit PS. These vesicles were then incubated for 1 hour at 37 °C with a known
250 amount of non-activated purified HAstV Yuc8. After incubation, the vesicles were
251 treated as described above (0.1% Triton X-100 for 30 minutes at 37˚C, anti-Yuc8
252 neutralizing antibody for 1 hour at 37°C or 0.1 % Triton X-100 followed by
253 neutralization with anti-Yuc8 antibody). After the treatments, vesicles with virus were
254 added to Caco-2 or MA104 cells grown in 96 wells, and incubated during 2 hours at
255 37°C. After this time cells were washed, and infection was left to proceed for 18
256 hours. As control, an equal amount of the identical purified trypsin activated or non-
257 activated astrovirus was used in the same conditions without EV incubation. Infected
258 cells were counted in selected area, of two wells per sample using 20X lens. Images
259 were acquired with 10X lens in a Nikon Diaphot 300 microscope.
260

261 **Transmission Electron Microscopy**

262 LEV and SEV vesicular fractions were purified from infected Caco-2 cells as
263 described above, using differential centrifugation coupled to isolation with the
264 MagCapture^{TM} exosome isolation kit PS. Purified fractions and non-activated purified
265 virus particles were bound on carbon vaporized copper grids covered with formvar
266 and negatively stained with 3% uranyl acetate. Images were acquired using a Zeiss
267 Libra 120 electron microscope operating at 80 KV coupled with a GATAN Multiscan
268 600HP 794 CCD camera.

bioRxiv preprint doi: https://doi.org/10.1101/2021.05.17.444590; this version posted May 18, 2021. The copyright holder for this preprint (which was not certified by peer review) is the author/funder. All rights reserved. No reuse allowed without permission.

269

270 **Nanoparticle Tracking Analysis**

271 Nanoparticle tracking analysis (NTA), was conducted using a NanoSight
272 NS300 (Malvern Instruments Ltd., Worcestershire, UK) to assess the hydrodynamic
273 diameter of non-activated virus particles and vesicles purified by differential
274 centrifugation from infected and non-infected cells supernatants. Purified fractions
275 were analyzed after diluting the samples in sterile and microfiltered PBS (1:100-200
276 in the case of vesicles and 1:1000 in case of purified virus particles). For each
277 condition 5 videos of one-minute length each, were recorded sizing 20-40
278 particles/frame and analyzed using the NanoSight NTA 3.1 software (43). This
279 technique uses dynamic light scattering to measure the diffusion coefficient of
280 particles moving under Brownian motion and converts it to hydrodynamic diameter
281 using the Stokes-Einstein equation (44). A blank of sterile filtered PBS was used for
282 particle calculations in every measurement, and after each measurement the
283 flushing lines were thoroughly washed three times to prevent contamination.

284

285 **Statistical Analysis**

286 Statistical analysis of the obtained results was performed using the GraphPad
287 prism 5.0 software (GraphPad Software, Inc.), with an interval of confidence of 95%.

288

289 **Results**

290 **HAstV Yuc8 titer in detergent-treated media increases with time of infection**

291 It has been previously observed that a fraction of the astrovirus particles
292 produced in infected cells floats to low-density fractions when separated by density
293 centrifugation, suggesting that they interact with membranous structures (14). To
294 characterize the possible association of astrovirus particles with membranes in the
295 cell culture media, we evaluated the kinetics of astrovirus release in Caco-2 cells.
296 Media from astrovirus infected cells were collected at different time points after
297 infection (from 12 to 24 hpi), and the virus titer was determined. The infectivity of the
298 virus in the supernatant was activated with trypsin after the samples were treated or
299 not with detergent (Triton X-100). Under these conditions, if astrovirus particles were

bioRxiv preprint doi: https://doi.org/10.1101/2021.05.17.444590; this version posted May 18, 2021. The copyright holder for this preprint (which was not certified by peer review) is the author/funder. All rights reserved. No reuse allowed without permission.

300 associated with vesicles or membranes, the detergent treatment would release the
301 virions, leading to an increase in viral titer as compared to the titer of samples not
302 treated with detergent. We observed the virus present in the supernatant starting at
303 the first time point analyzed (12 hpi), without any significant change in the titer after
304 Triton X-100 treatment ($p>0.05$) (Fig. 1), similar to previously published results (10).
305 The titer of virus present in the media not treated with detergent showed little
306 increase from 15 to 24 h post infection, however, the viral titer increased
307 considerably in the supernatant after detergent treatment, reaching almost twice as
308 much infectivity compared to non-treated samples, at later time points (Fig. 1). No
309 significant cellular damage was detected at the different time points (being under
310 10% of total LDH in both mock and Yuc8 infected cells), as determined by an LDH
311 assay (results not shown). These results suggest that astrovirus particles are
312 released from infected cells before appreciable cell lysis, and that they could be
313 associated with detergent soluble structures in the extracellular medium. In all the
314 subsequent experiments shown here, media were harvested at 18 hpi.
315
316 **Astrovirus infection increases the secretion of extracellular vesicles**
317 **from Caco-2 cells**
318 To characterize the effect of astrovirus infection on the production of EV in
319 Caco-2 cells, supernatants from infected or mock-infected cells cultured in serum-
320 free MEM were harvested at 18 hpi and processed by differential centrifugation.
321 Initially, detached cells were pelleted at 500 g for 5 min, getting pellet 1 (P1). Pellet
322 2 (P2) was obtained by centrifugation of the remaining supernatant at 2,000 g for 30
323 min. We expected this fraction to contain very large vesicles and some cell debris
324 and organelles. Pellet 3 was obtained by centrifugation of the remaining supernatant
325 at 20,000 g for 1 h, to collect large extracellular vesicles (LEV), theoretically
326 calculated to be over 122 nm (42). Finally, pellet 4 was obtained by overnight
327 precipitation of remaining vesicles and particles in the remaining supernatant by 8%
328 PEG 6000 and 0.5 M NaCl, followed by centrifugation at 10,000 g for 1 h, producing
329 small extracellular vesicles fraction (SEV), calculated to be under 170 nm (41, 42).
330 As consequence, we expect some size overlapping between LEV and SEV fractions.

bioRxiv preprint doi: https://doi.org/10.1101/2021.05.17.444590; this version posted May 18, 2021. The copyright holder for this preprint (which was not certified by peer review) is the author/funder. All rights reserved. No reuse allowed without permission.

331 An equal portion of each pellet fraction was analyzed after SDS-PAGE. By
332 silver staining of the gel, it was clear that the amount of total proteins present in each
333 fraction was increased in astrovirus-infected cells (Fig. 2A). The presence of different
334 cellular markers in the pelleted fractions was analyzed by immunoblotting; EV
335 specific markers tested were CD63 and ALIX, while endoplasmic reticulum
336 associated PDI protein was used as non-EV associated protein control. In fractions
337 P1 and P2, which probably contain cells, cell debris and large vesicles, all proteins
338 markers were observed, and their presence also has increased after astrovirus
339 infection. Interestingly, the LEV and SEV fractions purified from astrovirus-infected
340 Caco-2 cells showed a higher content of EV specific proteins (ALIX and CD63) as
341 compared to mock-infected cells (Fig. 2B), presumably representing larger amounts
342 of EVs. (Fig. 2B).

343 To quantitate the concentration and size of the purified vesicles more
344 precisely, the pellet 3 (LEV fraction) and the fraction purified after PEG 6000
345 precipitation (SEV fraction) were analyzed by nanoparticle tracking analysis (Fig. 3).
346 There was a clear and significative increase in the vesicle number in the LEV fraction
347 from Yuc8-infected cells ($p<0.05$), compared to that of mock-infected cells (Fig. 3A
348 and 3C). In the case of the SEV fraction obtained by PEG 6000 precipitation, there
349 was only a small, not significant increase ($p>0.05$) on the number of vesicles present
350 in preparations obtained from either infected cells or mock-infected cells (Fig. 3B
351 and 3C). These results suggest that astrovirus infection might stimulate the
352 production of EV, particularly those present in the LEV fraction.

353

354 **Astrovirus particles seem to associate with extracellular vesicles**

355 Given the presence of vesicles with different sizes in the cell culture medium,
356 we analyzed whether astrovirus particles were associated with a particular fraction
357 and if an increased infectivity could be observed after treating the different fractions
358 with Triton X-100 before activation of the virus with trypsin. We found that different
359 amounts of infectious viral particles were present in fractions P2, LEV, and SEV;
360 treatment with Triton X-100 before trypsin activation significantly increased virus titer
361 in fractions P2 ($p<0.05$) and LEV ($p<0.01$), but not in fraction SEV (Fig. 4A). These

bioRxiv preprint doi: https://doi.org/10.1101/2021.05.17.444590; this version posted May 18, 2021. The copyright holder for this preprint (which was not certified by peer review) is the author/funder. All rights reserved. No reuse allowed without permission.

362 observations suggest that a portion of the astrovirus particles could be present inside
363 vesicles or, alternatively, that groups of viral particles could be associated with EV
364 from the outside, and consequently membrane solubilization releases individual
365 particles, increasing virus titer.
366 To determine if there is a direct association between virions and vesicles in
367 the LEV fraction, we analyzed by transmission electron microscopy (TEM) this
368 fraction purified from astrovirus infected Caco2 cells. The LEV fraction was chosen
369 since the largest increase in virus infectivity when the trypsin activation was done
370 after the Triton X-100 treatment was observed in this fraction. By TEM we found
371 virus-like particles, associated with what appeared to be vesicles (Fig. 4B, pointed
372 by arrows). The electro-dense virus-like particles observed in this micrograph, are
373 similar in form and size (30 nm) to purified astrovirus particles (Fig. 4C), suggesting
374 that they represent bona-fide virus particles associated with membranes. Such virus-
375 like particles were not observed in vesicles present in LEV fraction purified from
376 mock-infected cells (data not shown). Since the infectivity of astroviruses requires
377 activation by proteolytic processing of the VP70 protein precursor, we analyzed by
378 western blot the virus protein composition of the LEV-associated virions. We
379 observed that the virus particles are mainly composed by the VP70 protein (70 KDa)
380 with no evidence of neither VP90 precursor protein, nor any activated viral proteins
381 of 34, 27 or 25 KDa proteins (Fig. 4D).
382

383 **Vesicle-associated astrovirus particles are infectious without**
384 **proteolytic treatment and are protected from antibody neutralization**

385 EVs have an intrinsic capacity to fuse with other cells, and thus to transfer
386 proteins, genetic material, and even viral particles to other recipient cells (16, 21, 24,
387 45). Using this mechanism, different types of viruses are able to infect otherwise
388 refractory cells. Such is the case of human immunodeficiency virus 1 (HIV-1) (46,
389 47) and herpes simplex virus 1 (HSV-1) (33). The association with vesicles has also
390 been shown to confer some viruses with resistance to neutralization with specific
391 antibodies [hepatitis A virus (HAV), or HSV-1] (33, 48). To test whether vesicle-
392 associated astrovirus strain Yuc8 is able to infect other cell lines, vesicles present in

bioRxiv preprint doi: https://doi.org/10.1101/2021.05.17.444590; this version posted May 18, 2021. The copyright holder for this preprint (which was not certified by peer review) is the author/funder. All rights reserved. No reuse allowed without permission.

393 the LEV and SEV fractions purified from infected Caco-2 cells were added to Caco-
394 2 and MA104 cells. Caco-2 cells were used as fully permissive cell line, while MA104
395 cells are at least 100 times less permissive to astrovirus Yuc8 infection (8, 49).
396 Before adding to the cell monolayers, the samples were either incubated with 0.1%
397 Triton X-100 for 1 h to disrupt possible membranes; or incubated with polyclonal
398 neutralizing polyclonal antibodies to Yuc8 to neutralize the infectivity of accessible
399 viral particles; or incubated with detergent followed by neutralization with the
400 neutralizing polyclonal antibodies in order to neutralize all viral particles present. As
401 control, fractions were only incubated in MEM.

402 The results of these assays show that the LEV and SEV vesicle-associated
403 astrovirus viral particles were able to infect both Caco-2 and MA104 cells (Fig. 5A
404 and B), while viral infection was completely abolished after membrane solubilization
405 with Triton X-100, suggesting that membranes or vesicles are indispensable for
406 infection, since astrovirus particles in these assays were not proteolytically activated.
407 Preincubation of both types of vesicles with anti-Yuc8 neutralizing polyclonal
408 antibody left a fraction of virus particles infectious, suggesting that some of these
409 viruses (10-20%) were protected from the neutralization by the antibodies, possibly
410 by being inside the vesicles (Fig. 5A, B and C). Accordingly, pretreatment of the
411 vesicle fractions with detergent, allowed complete antibody neutralization of the virus
412 particles (Fig. 5A and B), supporting the hypothesis that vesicles in these fractions
413 are important to allow viral infection and to shield viral particles from neutralizing
414 antibodies.

415 Protected viral particles were observed in both, LEV and SEV fractions, and
416 they were able to infect a similar number of both Caco-2 and MA104 cells (Fig. 5C).
417 When the infectivity was compared between Caco-2 and MA104 cells, Caco-2 cells
418 showed more infected cells by LEV fraction than MA104 cells, while infection
419 associated with SEV fraction was similar between both cell lines (Fig. 5C). In Caco-
420 2 cells there were more infected cells after infection with vesicles from LEV fraction,
421 as compared to SEV fraction, while in MA104 cells infectivity of these two fractions
422 was similar (Fig. 5C).

423

bioRxiv preprint doi: https://doi.org/10.1101/2021.05.17.444590; this version posted May 18, 2021. The copyright holder for this preprint (which was not certified by peer review) is the author/funder. All rights reserved. No reuse allowed without permission.

424 **Association of non-activated astrovirus Yuc8 with purified EVs**
425 **enhances viral infectivity**

426 To further evaluate the possibility that the association of the virus with
427 membranous structures promotes virus infectivity without the need of trypsin
428 treatment, non-activated purified Yuc8 particles were incubated for 1 h at 37 °C with
429 LEV and SEV fractions obtained from supernatants of mock-infected Caco-2 cells.
430 After virus-EV incubation, the virus-vesicle mixture was subjected to the same
431 treatments described in the previous experiment: neutralization with polyclonal anti-
432 Yuc8 antibody, membrane solubilization by incubation with 0.1% Triton X-100, or
433 detergent treatment followed by neutralization. Untreated virus-vesicle samples, in
434 MEM, were used as control. After treatment, the samples were added to Caco-2 and
435 MA104 monolayers and infection was left to proceed as described. The non-
436 activated astrovirus particles that were incubated with both types of purified vesicles
437 (LEV and SEV fractions) acquired the capacity to infect both Caco-2 and MA104
438 cells (Fig. 6A and B). Detergent treatment of the samples before addition to the cells
439 abolished the infectivity in both cell lines, again confirming the contribution of
440 membrane vesicles to viral infectivity of particles non-activated by trypsin, possibly
441 by direct interaction between virus and vesicles (Fig. 6A and B). Pre-incubation with
442 neutralizing antibodies abolished infectivity, suggesting that all viral particles were
443 accessible to the antibodies. Of note, no infection was detected when either cell line
444 was incubated with the same amount of non-activated virus, in the absence of
445 vesicles, unless the virus was activated by treatment with trypsin (Fig. 6C). As
446 expected, the combined treatment of detergent and neutralizing antibodies also
447 abolished the infection (Fig. 6A and B). These results suggest that free viral particles
448 could associate with vesicles, and this interaction facilitates their cell entry and
449 infectivity, even if the virus is not activated. When the infectivity of the vesicle-
450 associated non-activated astrovirus particles was compared in Caco-2 and MA104
451 cells, both LEV and SEV fractions showed similar capacity to promote infection in
452 both cell lines (Fig. 6C). Of interest, non-activated astrovirus particles incubated with
453 purified EV, infected MA104 cells more efficiently (>200%) than the same amount of
454 free virus activated with trypsin (Fig. 6C), while in Caco-2 cells (astrovirus fully

bioRxiv preprint doi: https://doi.org/10.1101/2021.05.17.444590; this version posted May 18, 2021. The copyright holder for this preprint (which was not certified by peer review) is the author/funder. All rights reserved. No reuse allowed without permission.

455 permissive cell line), the vesicle-associated particles had a 17% average infectivity
456 of the free, trypsin activated virus (Fig. 6C).
457

458 Discussion

459 Astrovirus cell release has been reported to be a non-lytic process promoted
460 by caspase processing of the viral capsid-precursor protein VP90 to VP70 (10, 11).
461 It is a gradual process in which the majority of the new particles (about 90% of the
462 total progeny) remain inside infected cells, and only 10% are released to the
463 extracellular media (10). In this study, we found that a portion of the new progeny
464 was present in the cell supernatant as early as 12 hpi and the amount of released
465 virus increased with time. Interestingly, starting at 15 hpi, a significant portion of the
466 released virus particles were not susceptible to trypsin treatment, and required to be
467 solubilized from their association with membranous structures by detergent
468 treatment, to become accessible to the protease. The amount of virus protected from
469 trypsin increased with time. This observation suggests that there could be more
470 potentially infectious virus particles in the extracellular media than originally thought
471 (10), most probably explained by the association of viruses with EVs.
472 Using differential centrifugation, we purified several fractions of EV from the
473 media of astrovirus Yuc8 infected Caco-2 cells, and two of these fractions were
474 characterized in more detail: the LEV fraction, obtained after cellular debris depletion
475 and by centrifugation for 1 h at 20,000 g; and the SEV fraction, purified after PEG
476 6000 based precipitation and centrifugation at 10,000 g (40, 42). Both fractions
477 contained markers of extracellular vesicles, CD63 and Alix. Since CD63 is an
478 specific marker of exosomes (50, 51), and ALIX has been reported to be involved in
479 both microvesicle and exosome biogenesis (45), it is possible that both of these
480 vesicles, which overlap in size, are present in both fractions. Analysis of the
481 concentration and size of the vesicles in LEV and SEV fractions by nanoparticle
482 tracking showed partial overlap in size, however the LEV fractions showed a
483 significative increase in the vesicle number when infected versus mock-infected
484 conditions were compared. A similar increase in EV secretion after infection was

bioRxiv preprint doi: https://doi.org/10.1101/2021.05.17.444590; this version posted May 18, 2021. The copyright holder for this preprint (which was not certified by peer review) is the author/funder. All rights reserved. No reuse allowed without permission.

485 also reported with other viruses, like HIV-1 (52, 53), HSV-1 (33, 54), rotavirus (27)
486 and tick-borne Langat virus (55).
487 Different viruses have been found to be able to interact directly with EV.
488 Among these, hepatitis A virus (HAV) (48), HCV (29), HSV-1 (33), and JC
489 polyomavirus (34). Analysis of the LEV fraction, purified from astrovirus-infected
490 cells, showed electrodense astrovirus-like particles associated with vesicles of about
491 200 nm, resembling the appearance of extracellular vesicles (56). The membranous
492 structures observed by TEM seem to associate with more than one viral particle.
493 This observation opens up the possibility that during astrovirus infection, EV could
494 participate both as virion carriers, protecting the virions, as well as a form of
495 concentrating viral particles, forming the so called collective infectious units (CIU),
496 capable to gather together several infectious particles. Similar observations have
497 been made recently for rotavirus and norovirus, where several viral particles were
498 reported to be associated with vesicles (27, 57).
499 It has been described previously that the association with vesicles could
500 protect some viruses from neutralization by antibodies, for example hepatitis A, B
501 and C viruses (29, 48, 58), and HSV-1 (33), among others. In this work we observed
502 that a portion of the astrovirus particles present in LEV and SEV fractions remained
503 infectious even after incubation with an anti-Yuc8 neutralizing antibody, suggesting
504 that a portion of the isolated astrovirus particles were inaccessible to the neutralizing
505 antibodies. The presence of vesicles was crucial for the infectivity of these non-
506 activated viral particles, since the solubilization of membranes with detergent
507 abrogated all infectivity. To confirm that vesicles are important in non-activated
508 astrovirus infectivity, LEV and SEV vesicles were purified from non-infected Caco-2
509 cells, and then incubated with non-trypsin activated purified astrovirus particles. Our
510 results showed that the purified virus, was able to interact with these vesicles, and
511 acquired the capacity to enter and infect the cells without protease activation. It is
512 not clear if these interactions between astrovirus particle and EVs interaction are
513 specific or not, but the virus particles in this mix acquired the capacity to infect even
514 low susceptibility cells like MA104. The infectivity was abolished by solubilization of
515 the vesicles with detergent, or by incubation with neutralizing antibodies, suggesting

bioRxiv preprint doi: https://doi.org/10.1101/2021.05.17.444590; this version posted May 18, 2021. The copyright holder for this preprint (which was not certified by peer review) is the author/funder. All rights reserved. No reuse allowed without permission.

516 that the interaction between viral particles and EV somehow facilitates the interaction
517 between the virus and the cell surface.

518 Since extracellular vesicles could facilitate the internalization of the virus
519 apparently through a viral receptor independent pathway, the viral particles
520 associated with vesicles could be internalized by a mechanism triggered by vesicles
521 themselves (59). The incubation of non-activated purified astrovirus with LEV or SEV
522 fractions leads to similar level of infection in both Caco-2 and MA104 cells, while
523 non-activated purified astrovirus particles were not able to infect these cell lines.
524 These results suggest that the astrovirus proteolytic processing by trypsin
525 (activation), is important for virus-cell adhesion and/or entry, but probably not for the
526 decapsidation process. The ability of astrovirus particles associated with vesicles to
527 infect not only susceptible Caco-2 cells, but also the poorly susceptible MA104 cell
528 line (Fig 6C), suggest that the vesicle-associated virus particles could bypass certain
529 blocks in astrovirus tropism, probably the specific virus-receptor interaction,
530 potentially increasing their pathogenicity. This observation also suggest that
531 extracellular vesicles could help astrovirus to disseminate outside the
532 gastrointestinal tract like it has been reported before for HAstV serotype 4 and the
533 novel astroviruses strains MLB and VA (2), possibly by allowing astroviruses to avoid
534 the immune response and cellular barriers until they get into permissive cells far
535 away from their common environment (gastrointestinal tract).

536 Our observations suggest the possibility that EV could be acting as platforms
537 to create collective infectious units (60, 61), rendering virus particles insensitive to
538 neutralization with antibodies and promoting their internalization in a non-receptor
539 dependent manner. The mechanisms by which EV promote viral internalization in
540 new cells remain unclear, as well as the contribution of EV to the whole astrovirus
541 infectivity.

542

543 **Acknowledgments**

544 This work was supported by grants 254608 and 302965 from CONACyT (Mexico).
545 We thank to Dra. Guadalupe Zavala for her assistance in transmission electron
546 microscopy. Carlos Baez-N was recipient of scholarship from CONACyT (Mexico),

bioRxiv preprint doi: https://doi.org/10.1101/2021.05.17.444590; this version posted May 18, 2021. The copyright holder for this preprint (which was not certified by peer review) is the author/funder. All rights reserved. No reuse allowed without permission.

547 No. 464741 for MS degree, and had support from the postgraduate studies program
548 (PAEP) of the National Autonomous University of Mexico (UNAM).

549

550 **References**

551

552 1. Meliopoulos V, Schultz-Cherry S. 2012. Astrovirus Pathogenesis., p 65-75. *In* Schultz-Cherry
553 S (ed), Astrovirus Research. Springer, New Yorl, NY.
554 2. Vu DL, Bosch A, Pinto RM, Guix S. 2017. Epidemiology of Classic and Novel Human
555 Astrovirus: Gastroenteritis and Beyond. Viruses 9.
556 3. Vu DL, Cordey S, Brito F, Kaiser L. 2016. Novel human astroviruses: Novel human diseases?
557 J Clin Virol 82:56-63.
558 4. Bosch A, Pinto RM, Guix S. 2014. Human astroviruses. Clin Microbiol Rev 27:1048-74.
559 5. E. M, Arias CF. 2013. Astroviruses, p 1347-1401. *In* Knipe DM (ed), Fields Virology, vol 2.
560 Lippincot Williams & Wilkins, Philadelpia.
561 6. Aguilar-Hernandez N, Meyer L, Lopez S, DuBois RM, Arias CF. 2020. Protein Disulfide
562 Isomerase A4 Is Involved in Genome Uncoating during Human Astrovirus Cell Entry. Viruses
563 13.
564 7. Arias CF, DuBois RM. 2017. The Astrovirus Capsid: A Review. Viruses 9.
565 8. Brinker JP, Blacklow NR, Herrmann JE. 2000. Human astrovirus isolation and propagation in
566 multiple cell lines. Arch Virol 145:1847-56.
567 9. Mendez E, Arias CF. 2013. Astroviruses, p 1347-1401. *In* Knipe DM (ed), Fields Virology.
568 Lippincot Williams and Wilkins, Philadephia.
569 10. Banos-Lara Mdel R, Mendez E. 2010. Role of individual caspases induced by astrovirus on
570 the processing of its structural protein and its release from the cell through a non-lytic
571 mechanism. Virology 401:322-32.
572 11. Mendez E, Salas-Ocampo E, Arias CF. 2004. Caspases mediate processing of the capsid
573 precursor and cell release of human astroviruses. J Virol 78:8601-8.
574 12. Aguilar-Hernandez N, Lopez S, Arias CF. 2018. Minimal capsid composition of infectious
575 human astrovirus. Virology 521:58-61.
576 13. Mendez E, Fernandez-Luna T, Lopez S, Mendez-Toss M, Arias CF. 2002. Proteolytic
577 processing of a serotype 8 human astrovirus ORF2 polyprotein. J Virol 76:7996-8002.
578 14. Mendez E, Aguirre-Crespo G, Zavala G, Arias CF. 2007. Association of the astrovirus
579 structural protein VP90 with membranes plays a role in virus morphogenesis. J Virol
580 81:10649-58.
581 15. Altan-Bonnet N, Chen YH. 2015. Intercellular Transmission of Viral Populations with Vesicles.
582 J Virol 89:12242-4.
583 16. Barteneva NS, Maltsev N, Vorobjev IA. 2013. Microvesicles and intercellular communication
584 in the context of parasitism. Front Cell Infect Microbiol 3:49.
585 17. Schorey JS, Cheng Y, Singh PP, Smith VL. 2015. Exosomes and other extracellular vesicles in
586 host-pathogen interactions. EMBO Rep 16:24-43.
587 18. Raposo G, Stoorvogel W. 2013. Extracellular vesicles: exosomes, microvesicles, and friends.
588 J Cell Biol 200:373-83.
589 19. Minciacchi VR, Freeman MR, Di Vizio D. 2015. Extracellular vesicles in cancer: exosomes,
590 microvesicles and the emerging role of large oncosomes. Semin Cell Dev Biol 40:41-51.

bioRxiv preprint doi: https://doi.org/10.1101/2021.05.17.444590; this version posted May 18, 2021. The copyright holder for this preprint (which was not certified by peer review) is the author/funder. All rights reserved. No reuse allowed without permission.

591 20. Thery C, Witwer KW, Aikawa E, Alcaraz MJ, Anderson JD, Andriantsitohaina R, Antoniou A,
592 Arab T, Archer F, Atkin-Smith GK, Ayre DC, Bach JM, Bachurski D, Baharvand H, Balaj L,
593 Baldacchino S, Bauer NN, Baxter AA, Bebawy M, Beckham C, Bedina Zavec A, Benmoussa A,
594 Berardi AC, Bergese P, Bielska E, Blenkiron C, Bobis-Wozowicz S, Boilard E, Boireau W,
595 Bongiovanni A, Borras FE, Bosch S, Boulanger CM, Breakefield X, Breglio AM, Brennan MA,
596 Brigstock DR, Brisson A, Broekman ML, Bromberg JF, Bryl-Gorecka P, Buch S, Buck AH,
597 Burger D, Busatto S, Buschmann D, Bussolati B, Buzas EI, Byrd JB, Camussi G, et al. 2018.
598 Minimal information for studies of extracellular vesicles 2018 (MISEV2018): a position
599 statement of the International Society for Extracellular Vesicles and update of the
600 MISEV2014 guidelines. J Extracell Vesicles 7:1535750.
601 21. Thery C, Ostrowski M, Segura E. 2009. Membrane vesicles as conveyors of immune
602 responses. Nat Rev Immunol 9:581-93.
603 22. Casorla-Perez LA, Lopez T, Lopez S, Arias CF. 2018. The Ubiquitin-Proteasome System Is
604 Necessary for Efficient Replication of Human Astrovirus. J Virol 92.
605 23. Karpe YA, Meng XJ. 2012. Hepatitis E virus replication requires an active ubiquitin-
606 proteasome system. J Virol 86:5948-52.
607 24. Kourembanas S. 2015. Exosomes: vehicles of intercellular signaling, biomarkers, and vectors
608 of cell therapy. Annu Rev Physiol 77:13-27.
609 25. Lai FW, Lichty BD, Bowdish DM. 2015. Microvesicles: ubiquitous contributors to infection
610 and immunity. J Leukoc Biol 97:237-45.
611 26. Altan-Bonnet N. 2016. Extracellular vesicles are the Trojan horses of viral infection. Curr
612 Opin Microbiol 32:77-81.
613 27. Isa P, Perez-Delgado A, Quevedo IR, Lopez S, Arias CF. 2020. Rotaviruses Associate with
614 Distinct Types of Extracellular Vesicles. Viruses 12.
615 28. Meckes DG, Jr. 2015. Exosomal communication goes viral. J Virol 89:5200-3.
616 29. Liu Z, Zhang X, Yu Q, He JJ. 2014. Exosome-associated hepatitis C virus in cell cultures and
617 patient plasma. Biochem Biophys Res Commun 455:218-22.
618 30. Nagashima S, Jirintai S, Takahashi M, Kobayashi T, Tanggis, Nishizawa T, Kouki T, Yashiro T,
619 Okamoto H. 2014. Hepatitis E virus egress depends on the exosomal pathway, with
620 secretory exosomes derived from multivesicular bodies. J Gen Virol 95:2166-2175.
621 31. Nagashima S, Takahashi M, Kobayashi T, Tanggis, Nishizawa T, Nishiyama T, Primadharsini
622 PP, Okamoto H. 2017. Characterization of the Quasi-Enveloped Hepatitis E Virus Particles
623 Released by the Cellular Exosomal Pathway. J Virol 91.
624 32. Tamai K, Shiina M, Tanaka N, Nakano T, Yamamoto A, Kondo Y, Kakazu E, Inoue J, Fukushima
625 K, Sano K, Ueno Y, Shimosegawa T, Sugamura K. 2012. Regulation of hepatitis C virus
626 secretion by the Hrs-dependent exosomal pathway. Virology 422:377-85.
627 33. Bello-Morales R, Praena B, de la Nuez C, Rejas MT, Guerra M, Galan-Ganga M, Izquierdo M,
628 Calvo V, Krummenacher C, Lopez-Guerrero JA. 2018. Role of Microvesicles in the Spread of
629 Herpes Simplex Virus 1 in Oligodendrocytic Cells. J Virol 92.
630 34. Morris-Love J, Gee GV, O'Hara BA, Assetta B, Atkinson AL, Dugan AS, Haley SA, Atwood WJ.
631 2019. JC Polyomavirus Uses Extracellular Vesicles To Infect Target Cells. mBio 10.
632 35. Mendez-Toss M, Romero-Guido P, Munguia ME, Mendez E, Arias CF. 2000. Molecular
633 analysis of a serotype 8 human astrovirus genome. J Gen Virol 81:2891-2897.
634 36. Oceguera A, Peralta AV, Martinez-Delgado G, Arias CF, Lopez S. 2018. Rotavirus RNAs
635 sponge host cell RNA binding proteins and interfere with their subcellular localization.
636 Virology 525:96-105.

bioRxiv preprint doi: https://doi.org/10.1101/2021.05.17.444590; this version posted May 18, 2021. The copyright holder for this preprint (which was not certified by peer review) is the author/funder. All rights reserved. No reuse allowed without permission.

637 37. Mendez E, Salas-Ocampo MP, Munguia ME, Arias CF. 2003. Protein products of the open
638 reading frames encoding nonstructural proteins of human astrovirus serotype 8. J Virol
639 77:11378-84.
640 38. Sanchez-Fauquier A, Carrascosa AL, Carrascosa JL, Otero A, Glass RI, Lopez JA, San Martin C,
641 Melero JA. 1994. Characterization of a human astrovirus serotype 2 structural protein
642 (VP26) that contains an epitope involved in virus neutralization. Virology 201:312-20.
643 39. Guerrero CA, Zarate S, Corkidi G, Lopez S, Arias CF. 2000. Biochemical characterization of
644 rotavirus receptors in MA104 cells. J Virol 74:9362-71.
645 40. Rider MA, Hurwitz SN, Meckes DG, Jr. 2016. ExtraPEG: A Polyethylene Glycol-Based Method
646 for Enrichment of Extracellular Vesicles. Sci Rep 6:23978.
647 41. Thery C, Amigorena S, Raposo G, Clayton A. 2006. Isolation and characterization of
648 exosomes from cell culture supernatants and biological fluids. Curr Protoc Cell Biol Chapter
649 3:Unit 3 22.
650 42. Livshits MA, Khomyakova E, Evtushenko EG, Lazarev VN, Kulemin NA, Semina SE, Generozov
651 EV, Govorun VM. 2015. Isolation of exosomes by differential centrifugation: Theoretical
652 analysis of a commonly used protocol. Sci Rep 5:17319.
653 43. Quevedo IR, O'sson ALJ, Clark RJ, Veinot JGC, Tufenkji N. 2014. Interpreting deposition
654 behavior of polydisperse surface-modified nanoparticles using QCM-D and sand-packed
655 columns. Environmental Engineering Science, 31:326-337.
656 44. Hassellow M, Kaegi R. 2009. Analysis and characterization of manufactured nanoparticles in
657 aquatic environments., p 211-266. *In* Lead JR, Smith E (ed), Environmental and human
658 health impacts of nanotechnology. Wiley, Chichester, West Sussex.
659 45. van Niel G, D'Angelo G, Raposo G. 2018. Shedding light on the cell biology of extracellular
660 vesicles. Nat Rev Mol Cell Biol 19:213-228.
661 46. Mack M, Kleinschmidt A, Bruhl H, Klier C, Nelson PJ, Cihak J, Plachy J, Stangassinger M, Erfle
662 V, Schlondorff D. 2000. Transfer of the chemokine receptor CCR5 between cells by
663 membrane-derived microparticles: a mechanism for cellular human immunodeficiency virus
664 1 infection. Nat Med 6:769-75.
665 47. Rozmyslowicz T, Majka M, Kijowski J, Murphy SL, Conover DO, Poncz M, Ratajczak J, Gaulton
666 GN, Ratajczak MZ. 2003. Platelet- and megakaryocyte-derived microparticles transfer
667 CXCR4 receptor to CXCR4-null cells and make them susceptible to infection by X4-HIV. AIDS
668 17:33-42.
669 48. Feng Z, Hensley L, McKnight KL, Hu F, Madden V, Ping L, Jeong SH, Walker C, Lanford RE,
670 Lemon SM. 2013. A pathogenic picornavirus acquires an envelope by hijacking cellular
671 membranes. Nature 496:367-71.
672 49. Aguilar-Hernandez N. 2018. Caracterizacion de las interacciones tempranas de astrovirus de
673 humano con celulas permisivas y resistentes a la infeccion. master. Universidad Nacional
674 Autonoma de Mexico.
675 50. Kalra H, Simpson RJ, Ji H, Aikawa E, Altevogt P, Askenase P, Bond VC, Borras FE, Breakefield
676 X, Budnik V, Buzas E, Camussi G, Clayton A, Cocucci E, Falcon-Perez JM, Gabrielsson S, Gho
677 YS, Gupta D, Harsha HC, Hendrix A, Hill AF, Inal JM, Jenster G, Kramer-Albers EM, Lim SK,
678 Llorente A, Lotvall J, Marcilla A, Mincheva-Nilsson L, Nazarenko I, Nieuwland R, Nolte-'t
679 Hoen EN, Pandey A, Patel T, Piper MG, Pluchino S, Prasad TS, Rajendran L, Raposo G, Record
680 M, Reid GE, Sanchez-Madrid F, Schiffelers RM, Siljander P, Stensballe A, Stoorvogel W,
681 Taylor D, Thery C, Valadi H, van Balkom BW, et al. 2012. Vesiclepedia: a compendium for
682 extracellular vesicles with continuous community annotation. PLoS Biol 10:e1001450.
683 51. Kowal J, Arras G, Colombo M, Jouve M, Morath JP, Primdal-Bengtson B, Dingli F, Loew D,
684 Tkach M, Thery C. 2016. Proteomic comparison defines novel markers to characterize

bioRxiv preprint doi: https://doi.org/10.1101/2021.05.17.444590; this version posted May 18, 2021. The copyright holder for this preprint (which was not certified by peer review) is the author/funder. All rights reserved. No reuse allowed without permission.

685 heterogeneous populations of extracellular vesicle subtypes. Proc Natl Acad Sci U S A
686 113:E968-77.
687 52. Arenaccio C, Chiozzini C, Columba-Cabezas S, Manfredi F, Affabris E, Baur A, Federico M.
688 2014. Exosomes from human immunodeficiency virus type 1 (HIV-1)-infected cells license
689 quiescent CD4+ T lymphocytes to replicate HIV-1 through a Nef- and ADAM17-dependent
690 mechanism. J Virol 88:11529-39.
691 53. Kulkarni R, Prasad A. 2017. Exosomes Derived from HIV-1 Infected DCs Mediate Viral trans-
692 Infection via Fibronectin and Galectin-3. Sci Rep 7:14787.
693 54. Deschamps T, Kalamvoki M. 2018. Extracellular Vesicles Released by Herpes Simplex Virus
694 1-Infected Cells Block Virus Replication in Recipient Cells in a STING-Dependent Manner. J
695 Virol 92.
696 55. Zhou W, Woodson M, Neupane B, Bai F, Sherman MB, Choi KH, Neelakanta G, Sultana H.
697 2018. Exosomes serve as novel modes of tick-borne flavivirus transmission from arthropod
698 to human cells and facilitates dissemination of viral RNA and proteins to the vertebrate
699 neuronal cells. PLoS Pathog 14:e1006764.
700 56. Rikkert LG, Nieuwland R, Terstappen L, Coumans FAW. 2019. Quality of extracellular vesicle
701 images by transmission electron microscopy is operator and protocol dependent. J Extracell
702 Vesicles 8:1555419.
703 57. Santiana M, Ghosh S, Ho BA, Rajasekaran V, Du WL, Mutsafi Y, De Jesus-Diaz DA, Sosnovtsev
704 SV, Levenson EA, Parra GI, Takvorian PM, Cali A, Bleck C, Vlasova AN, Saif LJ, Patton JT,
705 Lopalco P, Corcelli A, Green KY, Altan-Bonnet N. 2018. Vesicle-Cloaked Virus Clusters Are
706 Optimal Units for Inter-organismal Viral Transmission. Cell Host Microbe 24:208-220 e8.
707 58. Yang Y, Han Q, Hou Z, Zhang C, Tian Z, Zhang J. 2017. Exosomes mediate hepatitis B virus
708 (HBV) transmission and NK-cell dysfunction. Cell Mol Immunol 14:465-475.
709 59. McKelvey KJ, Powell KL, Ashton AW, Morris JM, McCracken SA. 2015. Exosomes:
710 Mechanisms of Uptake. J Circ Biomark 4:7.
711 60. Sanjuan R. 2017. Collective Infectious Units in Viruses. Trends Microbiol 25:402-412.
712 61. Sanjuan R. 2018. Collective properties of viral infectivity. Curr Opin Virol 33:1-6.

713

714 ## Figure legends

715 **Figure 1. Kinetics of astrovirus release from infected Caco-2 cells.** Caco-
716 2 cells were infected with astrovirus Yuc8 at MOI of 5 and supernatants were
717 collected at different time points post infection (from 12 to 24 hours). Viral titer was
718 determined with (grey bars) and without (white bars) 0.1% Triton X-100 treatment
719 before trypsin activation. The results represent the mean focus forming units (FFU)
720 per milliliter (mL) ± standard error of the mean of three independent experiments
721 done in duplicate. Statistical analysis was done with two-way ANOVA, p value
722 *<0.05; ** p<0.01, *** p<0.001.

723

724 **Figure 2. Identification of vesicular markers in vesicles purified from**
725 **Caco-2 cells.** Caco-2 cells were infected or mock-infected with astrovirus strain

bioRxiv preprint doi: https://doi.org/10.1101/2021.05.17.444590; this version posted May 18, 2021. The copyright holder for this preprint (which was not certified by peer review) is the author/funder. All rights reserved. No reuse allowed without permission.

726 Yuc8 (MOI 5) and 18 hours post infection the supernatant was collected. Different
727 fractions were purified by differential centrifugation; pellet 1 was obtained by
728 centrifugation at 500 g (P1), pellet 2 obtained by centrifugation at 2,000 g (P2),
729 fraction containing large extracellular vesicles (LEV) was obtained after 20,000 g
730 centrifugation and final small extracellular vesicles (SEV) fraction was obtained by
731 precipitation with 8% polyethylene glycol 6000, 0.5M NaCl. (A) The same volume of
732 each pelleted fraction was separated by SDS-PAGE and proteins were detected by
733 silver staining. (B) Samples were resolved on SDS-PAGE and analyzed by western
734 blotting, using antibodies specific for CD63 and Alix as vesicle markers and protein
735 disulfide isomerase (PDI) as endoplasmic reticulum protein to assess preparation
736 contamination. Immunoblots are representative of five independent experiments.

737 **Figure 3. Astrovirus Yuc8 infection stimulates secretion of extracellular**
738 **vesicles in Caco-2 cells.** Confluently grown Caco-2 cells were infected with
739 astrovirus Yuc8 (MOI 5) or mock infected. Supernatants were harvested 18 hours
740 post infection and processed by differential centrifugation. Fractions obtained after
741 pelleting at 20,000 g, corresponding to large extracellular vesicles (LEV) (A) and
742 obtained after PEG 6000 precipitation, small extracellular vesicles (SEV) (B), were
743 resuspended in PBS and used for nanoparticle tracking analysis in the NanoSight
744 NS300. In each experiment five videos were recorded and used for analysis.
745 Distribution of particle-vesicle size (hydrodynamic diameter in nm) and concentration
746 (particles/mL) from 3 to 5 independent experiments are shown. Vesicles purified
747 from mock infected cells are represented by blue line, Yuc8 purified vesicles are
748 represented by red line. (C) Comparison of the mean number of particles present in
749 LEV and SEV fractions shown in A and B. All results are expressed as the mean of
750 the whole concentration of particles ± standard error of the mean of three
751 independent experiments. Statistical analysis was done using two-way ANOVA *
752 $p<0.05$.

753 **Figure 4. Astrovirus particles associate with large extracellular vesicles.**
754 Confluently grown Caco-2 cells were infected with astrovirus Yuc8 (MOI 5) or mock
755 infected. Supernatants were harvested 18 hours post infection and processed by
756 differential centrifugation. Fraction pellet 2 was obtained by centrifugation at 2,000 g

bioRxiv preprint doi: https://doi.org/10.1101/2021.05.17.444590; this version posted May 18, 2021. The copyright holder for this preprint (which was not certified by peer review) is the author/funder. All rights reserved. No reuse allowed without permission.

757 (P2), fraction containing large extracellular vesicles (LEV) was obtained after
758 centrifugation at 20,000 g and final small extracellular vesicles (SEV) fraction was
759 obtained by precipitation with PEG 6000, and NaCl after centrifugation at 10,000 g.
760 All fractions were resuspended in same volume (100 µL) of sterile PBS. (A) Purified
761 fractions were trypsin activated, with or without previous incubation with detergent,
762 and titered in Caco-2 cells. Viral content was expressed as total focus forming units.
763 Grey bars represent samples treated with 0.1% Triton X-100 prior trypsin activation;
764 white bars (MEM), represent samples activated with trypsin without Triton X-100
765 treatment. The mean of viral particles in each sample ± standard error of the mean
766 of three independent experiments are shown. (B) Large extracellular vesicles
767 purified from Yuc8 infected Caco-2 cells as described in A were further clarified by
768 additional isolation using MagCapture^{TM} Exosome Isolation kit PS. One drop of
769 sample was fixed onto carbon vaporized coper grids and negative stained with uranyl
770 acetate. Samples were observed in EFTEM ZEISS Libra 120 electron microscope.
771 Electrodense particles of 30 nm, possibly viral particles, are pointed by black arrows.
772 (C) Purified Yuc8 virions were bound to carbon vaporized coper grids and stained
773 as described in B. Electrodense particles, which resemble astrovirus particles are
774 pointed by arrows. Size bars are shown. (D) Immunoblotting of LEV fraction. Sample
775 used in A, purified from Caco-2 infected cells as described in A, was not-treated
776 (lane 1) or treated (lane 2) with trypsin, and separated in SDS-PAGE, transferred to
777 nitrocellulose membrane and viral proteins were detected using anti-astrovirus
778 polyclonal antibody. Viral proteins are pointed on right hand side, while molecular
779 weight in kilodaltons is shown on left hand side. Images are representative of three
780 independent experiments yielding similar results. Statistical analysis was done with
781 two-way ANOVA, p value *<0.05; ** p<0.01, *** p<0.001.

782 **Figure 5. Vesicle associated astrovirus is infective in Caco-2 and MA104**
783 **cells.** Large extracellular vesicles (LEV) and small extracellular vesicles (SEV) were
784 purified by differential centrifugation and MagCapture^{TM} exosome isolation kit PS
785 from supernatants of Caco-2 cells infected with astrovirus (strain Yuc8). Samples
786 were treated with medium (MEM); 0.1% Triton X-100; anti-Yuc8 (1:1500); or 0.1%
787 Triton X-100 followed by anti-Yuc8 (1:1500) before addition to (A) Caco-2 or (B)

bioRxiv preprint doi: https://doi.org/10.1101/2021.05.17.444590; this version posted May 18, 2021. The copyright holder for this preprint (which was not certified by peer review) is the author/funder. All rights reserved. No reuse allowed without permission.

788 MA104 cells. Treated samples were let to adsorb for two hours, after which time
789 unbound vesicles were washed and infection was left to proceed for 18 hours.
790 Infected cells were detected by immuno-peroxidase staining (darker cells). Cells
791 were observed in a Nikon Diaphot 300 microscope with 10X magnification and they
792 are representative of three independent experiments done in three wells each. (C)
793 Focus forming units (FFU) of each sample were counted in 3 wells of three
794 independent experiments. Bars represent the viral focus forming units (FFU) in each
795 sample ± standard error of the mean. Samples where 0 FFU were observed (Triton
796 X-100 and Triton X-100 plus anti-Yuc8 treatments) are not graphically represented.
797 Statistical analysis was done with two-way ANOVA, p value *<0.05; ** p<0.01, ***
798 p<0.001.
799
800 **Figure 6. The interaction of non-activated astrovirus Yuc8 with vesicles**
801 **enhances their infectivity**
802 Large extracellular vesicles (LEV) and small extracellular vesicles (SEV) were
803 purified by differential centrifugation and MagCapture^{TM} exosome isolation kit PS
804 from supernatants of non-infected Caco-2 cells. Purified vesicles were incubated
805 with purified non-activated astrovirus Yuc8 particles for 1 hour at 37°C. Vesicle-virus
806 mixtures were treated in 4 different conditions: medium (MEM); 0.1% Triton X-100;
807 anti-Yuc8 (1:1500); and 0.1% Triton X-100 followed by anti-Yuc8 (1:1500). Treated
808 fractions were then let to adsorb in (A) Caco-2 or (B) MA104 cells for two hours, after
809 which time the unbound vesicles and viral particles were washed out. After 18 hpi
810 infected cells were detected by immuno-peroxidase staining (darker cells). Images
811 magnified with a 10X lens were observed in a Nikon Diaphot 300 microscope and
812 they are representative of three independent experiments done in triplicate. (C)
813 Infected cells observed in experimetns described in A and B were counted in three
814 wells of three independent experiments and compared with the same amount of
815 trypsin activated (Yuc8 Act) and non-activated (Yuc8 NA) astrovirus probed without
816 pre-incubation with EV in Caco-2 and MA104 cells. Graphics shown the amount of
817 infected cell in each sample expressed as focus forming units (FFU). Bars represent

bioRxiv preprint doi: https://doi.org/10.1101/2021.05.17.444590; this version posted May 18, 2021. The copyright holder for this preprint (which was not certified by peer review) is the author/funder. All rights reserved. No reuse allowed without permission.

818 the mean FFU ± standard error of the mean. Statistical analysis was done with two-
819 way ANOVA, p value *<0.05; ** p<0.01, *** p<0.001.
820
821
822
823
824
825
826
827
828
829
830
831
832
833
834
835
836
837
838
839
840
841
842
843
844
845
846
847
848

bioRxiv preprint doi: https://doi.org/10.1101/2021.05.17.444590; this version posted May 18, 2021. The copyright holder for this preprint (which was not certified by peer review) is the author/funder. All rights reserved. No reuse allowed without permission.

849 **Figures**

850

851 Figure 1.

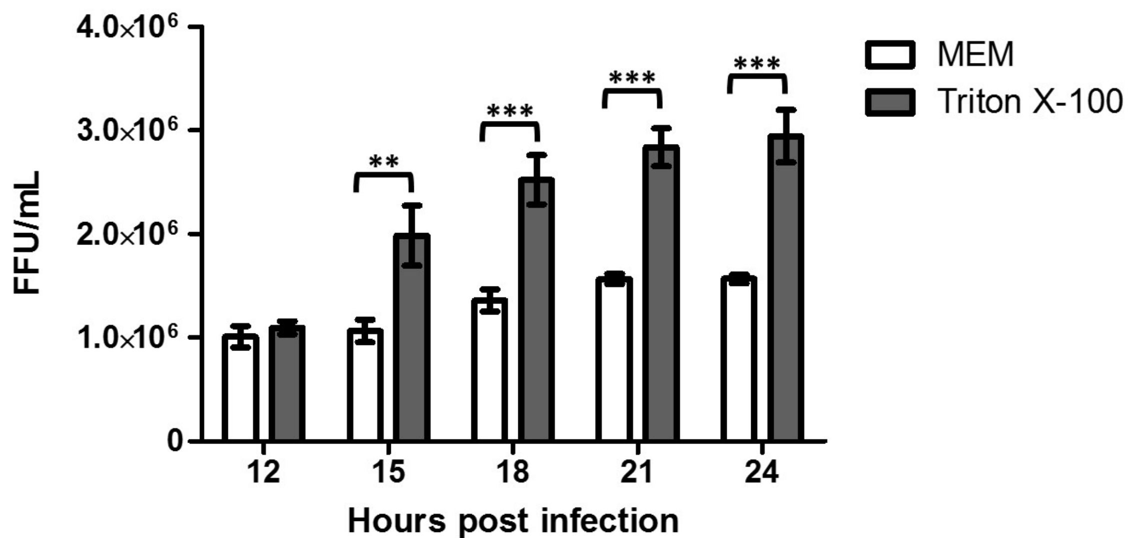

852
853
854
855
856
857
858
859
860
861
862
863
864
865
866
867
868

bioRxiv preprint doi: https://doi.org/10.1101/2021.05.17.444590; this version posted May 18, 2021. The copyright holder for this preprint (which was not certified by peer review) is the author/funder. All rights reserved. No reuse allowed without permission.

869 Figure 2.

870 A.

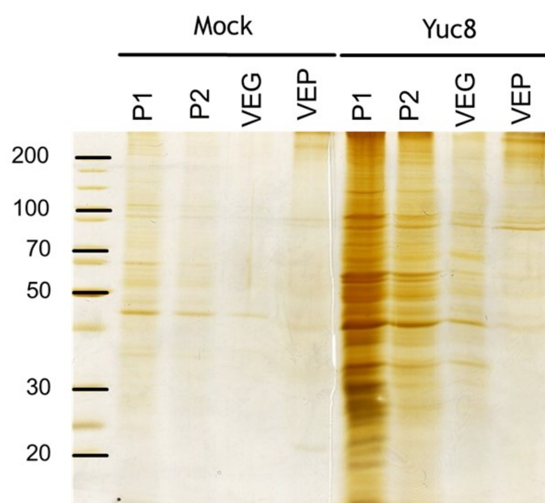

871

872 B.

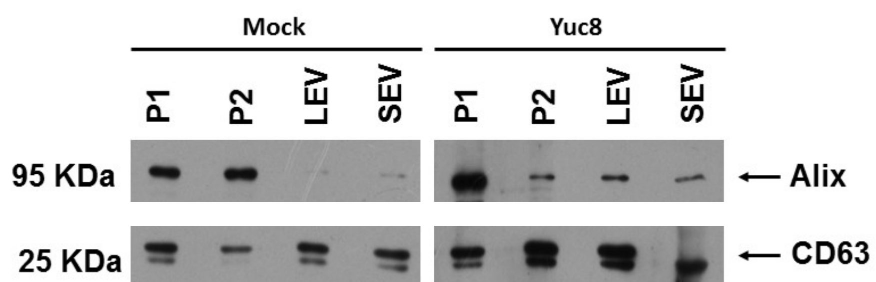

873

874

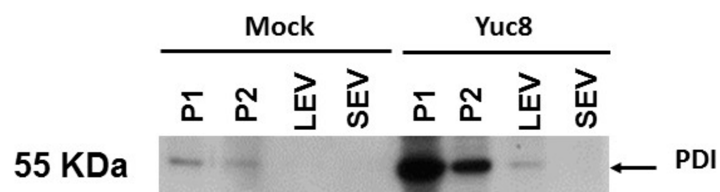

875

876

877

878

879

880

881

bioRxiv preprint doi: https://doi.org/10.1101/2021.05.17.444590; this version posted May 18, 2021. The copyright holder for this preprint (which was not certified by peer review) is the author/funder. All rights reserved. No reuse allowed without permission.

882 Figure 3.

883 A.

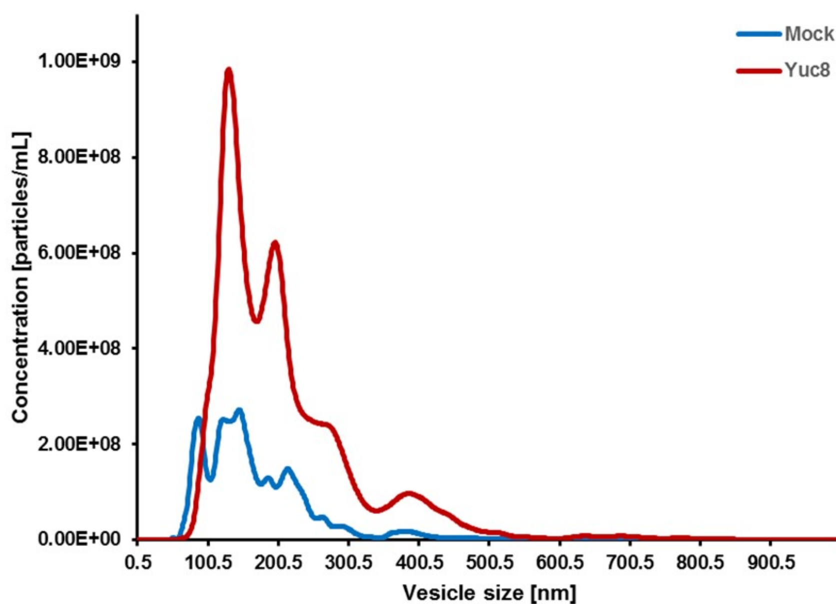

884

885 B.

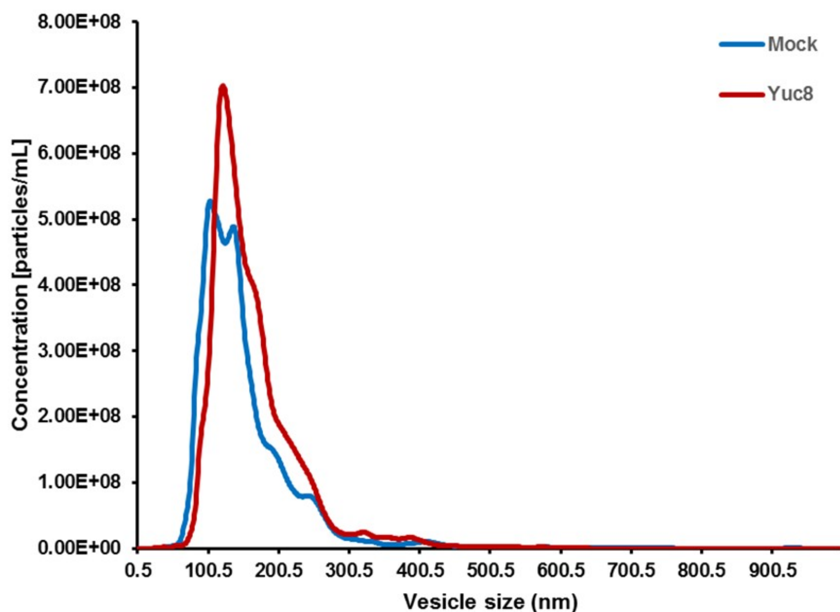

886

887

888

889

890

bioRxiv preprint doi: https://doi.org/10.1101/2021.05.17.444590; this version posted May 18, 2021. The copyright holder for this preprint (which was not certified by peer review) is the author/funder. All rights reserved. No reuse allowed without permission.

891 C.

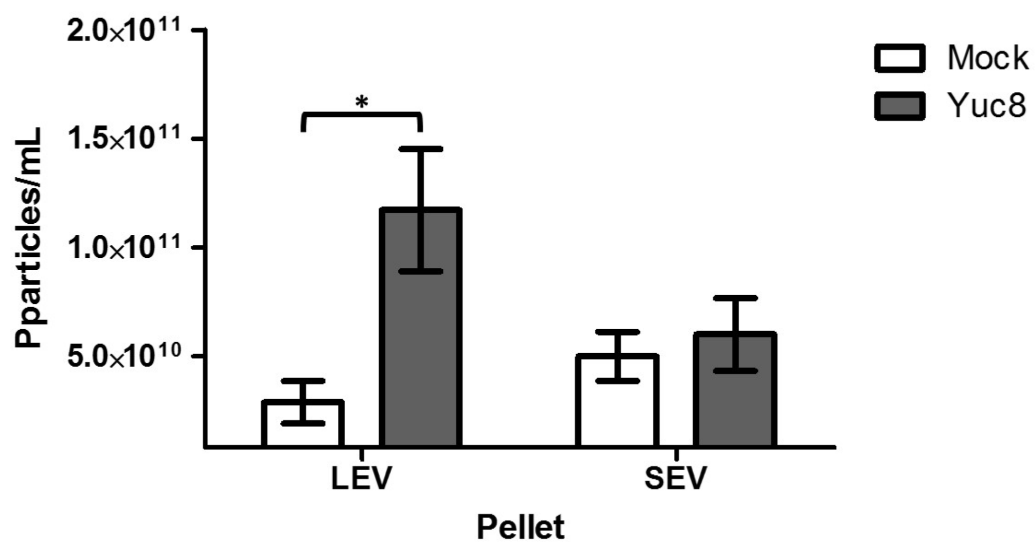

892
893
894
895
896
897
898
899
900
901
902
903
904
905
906
907
908
909
910

bioRxiv preprint doi: https://doi.org/10.1101/2021.05.17.444590; this version posted May 18, 2021. The copyright holder for this preprint (which was not certified by peer review) is the author/funder. All rights reserved. No reuse allowed without permission.

911

912 Figure 4.

913 A.

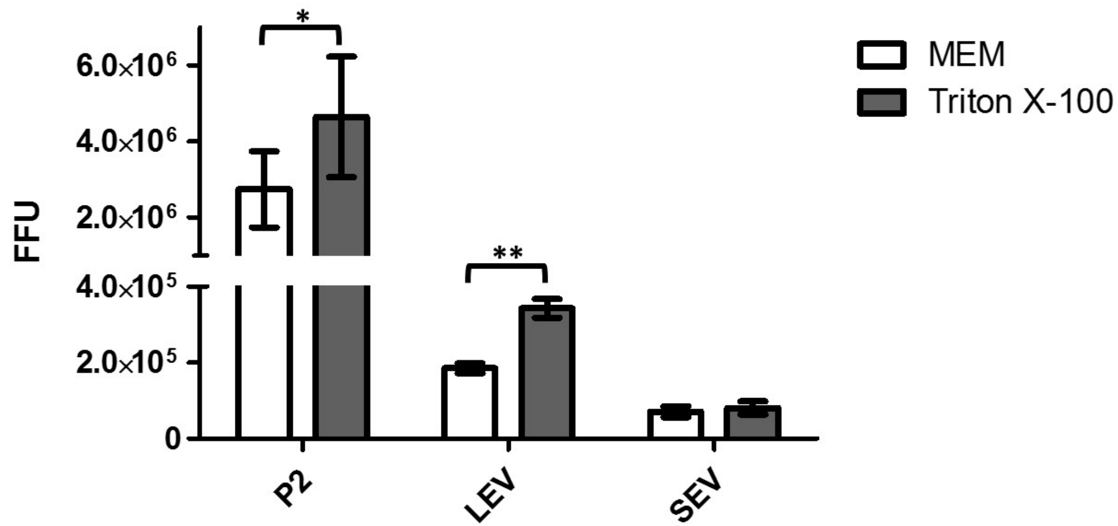

914

915 B.

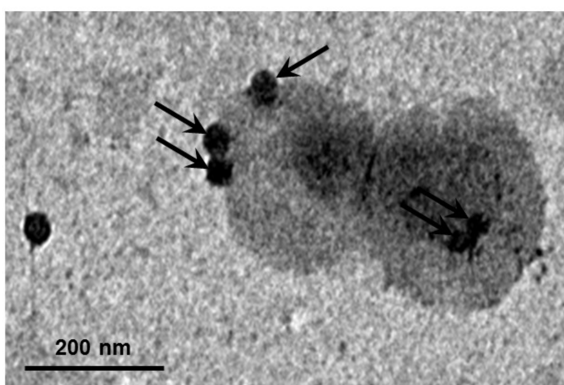

916

917

918

919

920

921

922

923

924

bioRxiv preprint doi: https://doi.org/10.1101/2021.05.17.444590; this version posted May 18, 2021. The copyright holder for this preprint (which was not certified by peer review) is the author/funder. All rights reserved. No reuse allowed without permission.

925 C.

926

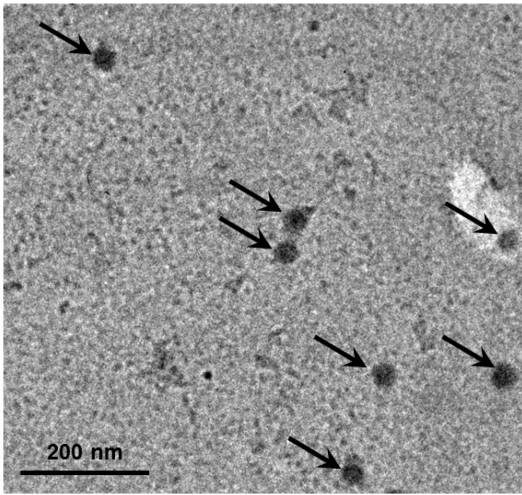

927

928

929

930

931

932 D.

933

934

935

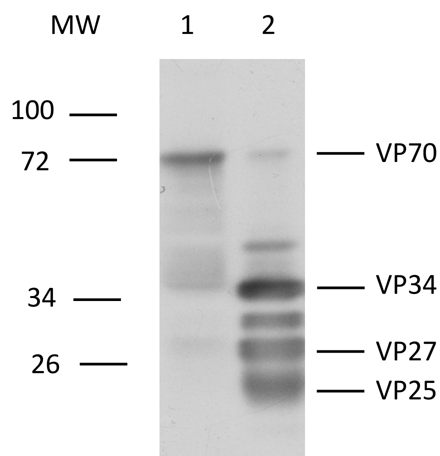

936

937

938

939

940

941

942

943

944

945

bioRxiv preprint doi: https://doi.org/10.1101/2021.05.17.444590; this version posted May 18, 2021. The copyright holder for this preprint (which was not certified by peer review) is the author/funder. All rights reserved. No reuse allowed without permission.

946 Figure 5.

947 A.

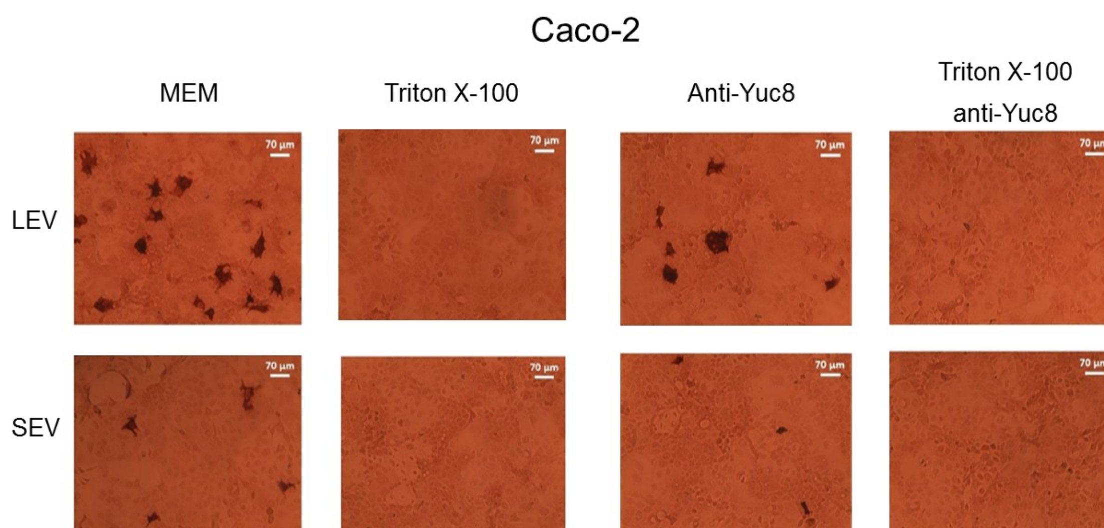

948

949 B.

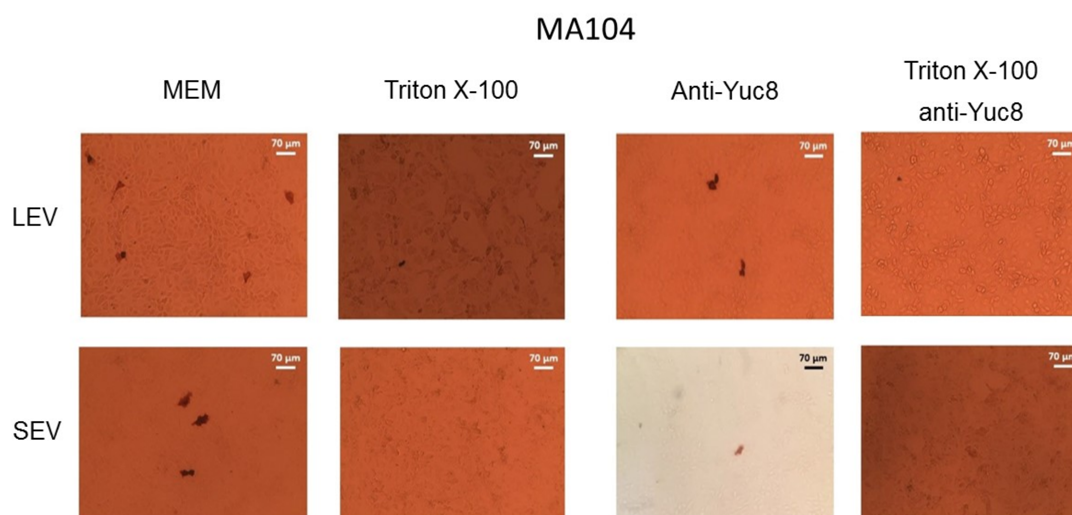

950
951
952
953
954
955
956
957

bioRxiv preprint doi: https://doi.org/10.1101/2021.05.17.444590; this version posted May 18, 2021. The copyright holder for this preprint (which was not certified by peer review) is the author/funder. All rights reserved. No reuse allowed without permission.

958 C.

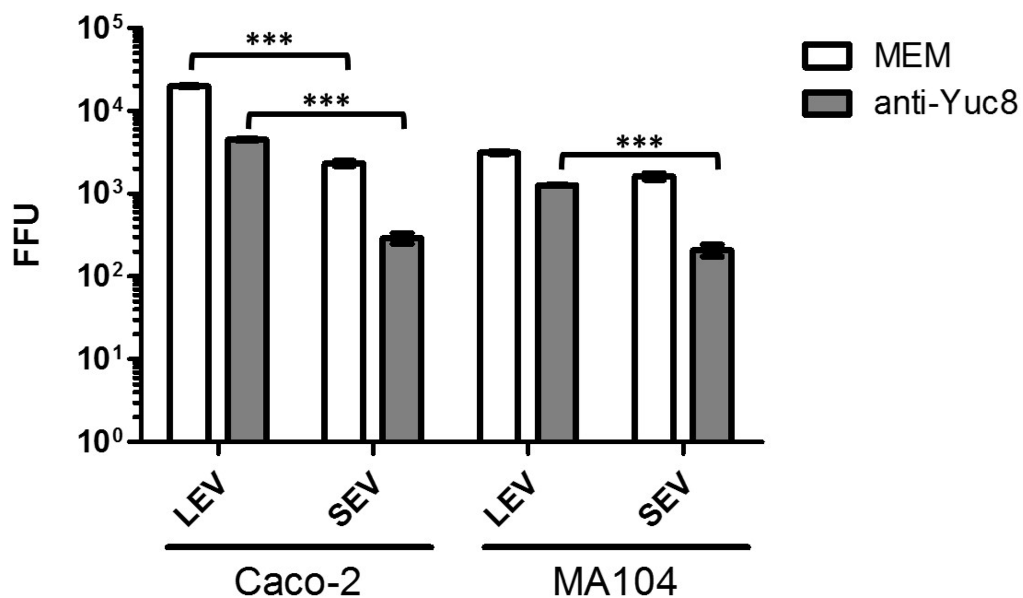

959
960
961
962
963
964
965
966
967
968
969
970
971
972
973
974
975

bioRxiv preprint doi: https://doi.org/10.1101/2021.05.17.444590; this version posted May 18, 2021. The copyright holder for this preprint (which was not certified by peer review) is the author/funder. All rights reserved. No reuse allowed without permission.

976 Figure 6.

977 A.

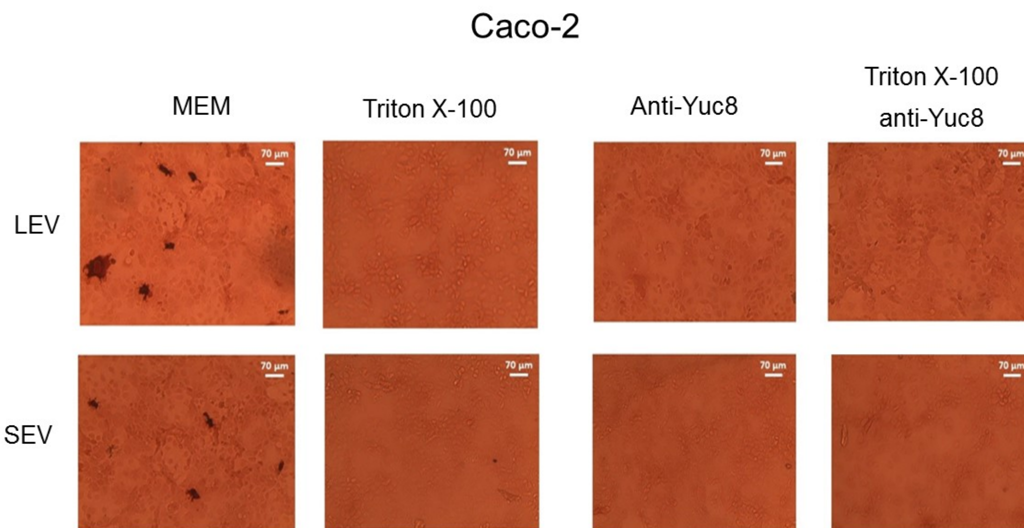

978

979 B.

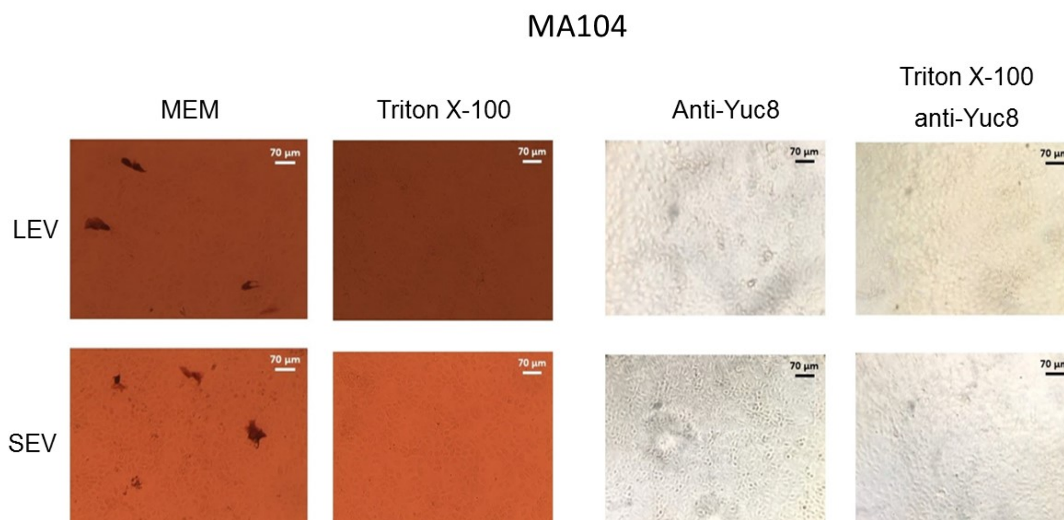

980

981

982

983

984

985

986

987

bioRxiv preprint doi: https://doi.org/10.1101/2021.05.17.444590; this version posted May 18, 2021. The copyright holder for this preprint (which was not certified by peer review) is the author/funder. All rights reserved. No reuse allowed without permission.

988 C.

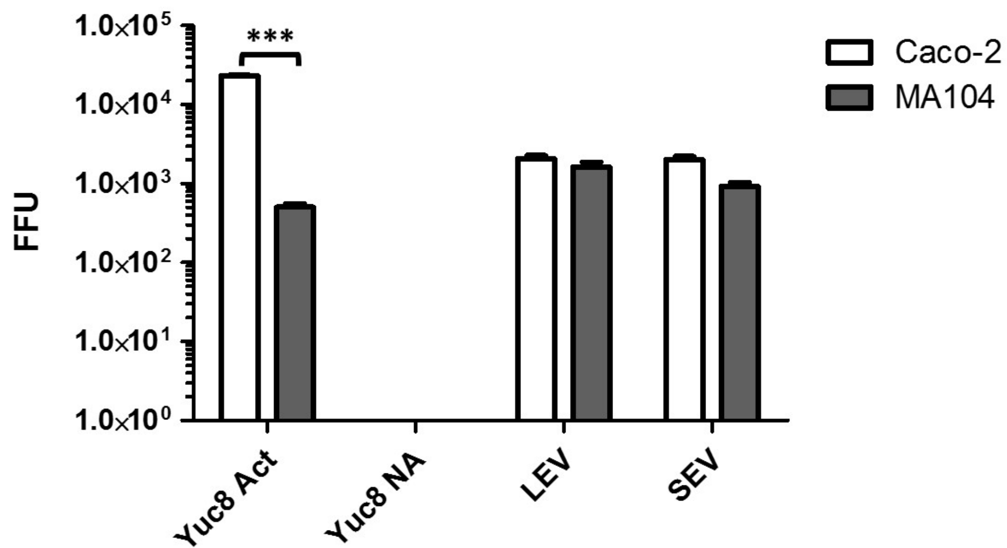

989
990
991
992
993
994
995
996
997
998